Design and Comparison of Two Advanced Driving Assistance Systems for the Lane Keeping in Intelligent Vehicles, based on LPV /H ∞ and Super-Twisting Sliding Mode (ST SM) Control Techniques

Alex Hamdan, Reine Talj, Véronique Cherfaoui

Design and Comparison of Two Advanced Driving Assistance Systems for the Lane Keeping in Intelligent Vehicles, based on $LPV/\mathscr{H}_\infty$ and Super-Twisting Sliding Mode ($STSM$) Control Techniques

Alex Hamdan[1], Reine Talj[1] and Véronique Cherfaoui[1]

***Abstract*— Active safety is an important issue that should be considered while driving on the road. To deal with this topic, this paper develops two Advanced Driving Assistance systems (*ADASs*) for the Lane Keeping in Intelligent Vehicles using steer-by-wire system. The objective of these systems (*ADASs*) is to assist the driver and help him to keep the lane and to ensure road safety. To do that, a new architecture of *ADAS* system is developed including the different Driving modes and a Fusion block. The Fusion Block permits the fusion of two inputs of the driver and the *ADAS* system respectively. Then, the $LPV/\mathscr{H}_\infty$ and the Super-Twisting Sliding Mode ($STSM$) control techniques are used for the development of *ADAS* controllers. A decision making layer monitors the driver's behavior and sends instantly the value of the fusion parameter that represents the assistance's percentage, according to the driving situation. The proposed *ADAS* systems are validated on Matlab/Simulink for a defined scenario with a complete nonlinear model of the vehicle validated on "*SCANeR Studio*" (OKtal) professional simulator. Finally, a comparison is done between both *ADAS* controllers to show the difference in behavior and performance of both strategies of control and the effectiveness of *ADAS* systems in the assistance objective while ensuring road safety.**

Keywords: Intelligent vehicle, *ADAS*, Lane keeping, $LPV/\mathscr{H}_\infty$ control, Super-Twisting Sliding Mode ($STSM$) control, Decision-making, Human-machine cooperative control.

I. INTRODUCTION

Autonomous driving has become a purposeful target for automotive companies as well as for research institutes in the recent years. For that, in 2013, the US Department of Transportation "National Highway Traffic Safety Administration NHTSA" classified the automation driving to many levels: from 0 to 5, to characterize their capabilities [1]. These levels start at offering some assistance features and end at realizing a full-autonomous vehicle passing by the semi-autonomous ones. Level 2 of automation consists of assisting the driver by several automated functionalities especially for active safety purpose. These systems are called Advanced Driving Assistance Systems (*ADASs*). They are integrated in the vehicle to protect the passengers in case of accident. There are the Passive systems (air bags, seat belts, etc.), and the Active systems that help and assist the driver in some driving tasks especially when he is tired or distracted (Lane keeping system, Emergency braking, Lane departure avoidance, etc.). Moreover, the development of electronics and sensors devices (LIDAR, GPS, etc.) supports the integration of these systems into the vehicle. The authors in [2] classified the *ADAS* systems to many categories based on their different types, uses and limitations, etc. Furthermore, many advanced studies are presented in the literature to deal with the development of these systems especially the Lane Keeping System. A linear Quadratic Regulator (*LQR*) control method is presented in [3] to develop the steering assist controller. A decision algorithm based on the lateral error deviation is used to determine the assistance and manage the control authority between the driver and the controller. The authors in [4] have developed a shared steering controller for lane keeping maneuver. The computation of the assistance system's control input is done considering the driver's activity and behavior in order to manage conflict between both agents. An assistance steer-by-wire system is developed in [5], where the driver's availability of the monitoring system is considered in the fusion of two steering inputs. The authors in [6] applied the H_2 control approach to calculate the assistance torque by using a first order filter coordination variable. A weighting approach presented in [7] is used to blend the two control inputs by using a fusion parameter α adjusted manually or automatically depending on the driving situations. A similar approach is developed in [8] to assist the driver during a lane following in case of tire blowout. Many factors are considered in the computation of α, such as: avoidance of lane departure, excessive steering, etc. The main difference between the presented works cited above is how to determine the fusion parameter α in order to realize the assistance objective. All these interesting studies have motivated us to design an Advanced Driving Assistance System (*ADAS*) for the lane keeping purpose using steer-by-wire system. However, this method can be adapted to overcome more complex maneuvers. Thus, in the present work, a new architecture of the Advanced Driving Assistance System given in the Fig. 1 is developed, to assist the driver in an intuitive way with high performance and efficiency during a lane keeping maneuver. The paper's contributions are illustrated in:

- The development of two *ADAS* systems controllers by using: the $LPV/\mathscr{H}_\infty$ and the Super-Twisting Sliding Mode ($STSM$) control techniques respectively.
- The development of a decision layer based on the driver's behavior for the assistance's percentage computation.
- The comparison between both *ADAS* controllers in terms of effectiveness and performance of each control technique.

[1]Université de Technologie de Compiègne, CNRS, Heudiasyc, CS 60 319, 60 203 Compiègne, France. Email: alex.hamdan@hds.utc.fr

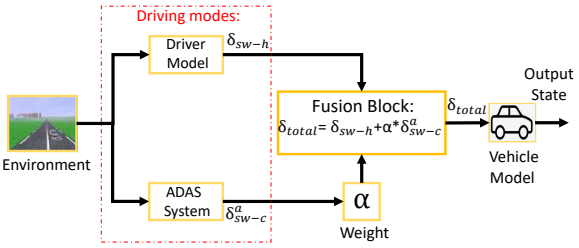

Fig. 1: Architecture of the Advanced Driving Assistance System.

The paper structure is as follow: in Section II a vehicle bicycle model is given for the control synthesis. The *ADAS* system architecture is presented in Section III including the Fusion Block and the Driving modes. A full description of the two *ADAS* systems based on the $LPV/\mathscr{H}_\infty$ and the Super-Twisting Sliding Mode (*STSM*) control techniques is introduced in Sections IV and V respectively. For that, the different layers: the control, the decision and the actuator layers are developed to realize the assistance objective based on the driver's behavior. Then, in Section VI, the simulation results and analysis for a given scenario are described to show the performance of both proposed *ADAS* systems. Validation of the developed *ADAS* systems is done on Matlab/Simulink, where a comparison is presented between both control approaches. Finally, the conclusions and the perspectives for future work are given in Section VII.

II. Control Synthesis Model

The vehicle bicycle model is a simplified version of the full vehicle model. It is an *LPV* model, with two variables being the vehicle side-slip angle β and the yaw rate $\dot{\psi}$. This model is usually used for model-based control synthesis to suit such control problem and it is given by the following system:

$$Plant\ P: \begin{cases} \dot{\beta} = -\frac{C_f+C_r}{mV_x}\beta - (1+\frac{l_fC_f-l_rC_r}{mV_x^2})\dot{\psi} \\ \qquad\qquad +\frac{C_f}{mV_x}\delta_{sw-c}, \\ \ddot{\psi} = -\frac{l_fC_f-l_rC_r}{I_z}\beta - \frac{l_f^2C_f+l_r^2C_r}{I_zV_x}\dot{\psi} \\ \qquad\qquad +\frac{l_fC_f}{I_z}\delta_{sw-c}, \end{cases} \tag{1}$$

where β and $\dot{\psi}$ are respectively the vehicle side-slip angle and the vehicle yaw rate. m is the vehicle mass, $l_{f,r}$ are the distances from the vehicle center of gravity to the front and rear axles respectively, $C_{f,r}$ are the front and rear tire cornering stiffness, I_z is the vehicle yaw moment of inertia, V_x is the vehicle longitudinal speed and finally δ_{sw-c} is the steering angle. This model is used for control synthesis of assistance system, for trajectory tracking purpose, when neglecting human input. Even though these equations are valid when the vehicle operates in the stable region, they are sufficient and recommended to synthesize a robust controller. The state space representation of the *Plant P* can be formalized as in (2), where $X = [\beta, \dot{\psi}]^T$ is the state vector, $U = [\delta_{sw-c}]^T$ is the control input.

III. *ADAS* System Architecture

Fig. 1 shows the block diagram of the Advanced Driving Assistance System (*ADAS*) architecture developed in the following to realize the lane keeping. The main components are: the Fusion Block and the Driving modes detailed in the following.

A. Fusion Block

The aim of the Fusion Block is to calculate the final steering wheel angle to the vehicle model. The total steering wheel angle in the case of *STSM ADAS* system, is given as:

$$\delta_{total} = \delta_{sw-h} + \alpha * \delta^a_{sw-c} \tag{3}$$

where δ_{total}, δ_{sw-h} and δ^a_{sw-c} are the total steering wheel angle, steering wheel angles of human driver and *ADAS* system respectively. α is an external parameter representing the assistance's percentage added by the driving assistance system to the driver's input. α is bounded in [0,1], calculated depending on a decision layer developed later. $\alpha = 1$ for full assistance and $\alpha = 0$ for zero assistance. However, in the case of $LPV/\mathscr{H}_\infty$ *ADAS* system, the total steering wheel angle is given as: $\delta_{total} = \delta_{sw-h} + \delta^a_{sw-c}$, where α is implicitly expressed in δ^a_{sw-c} through a scheduling gain ρ discussed later.

B. Driving Modes

1) Driver Model: the developed Driver Model in [9] is used to represent the human driver in-the-loop. His steering input will be noted as δ_{sw-h}.

2) ADAS System: the *ADAS* system is a controller developed to assist the driver and help him during a lane following maneuver depending on his behavior. Two control techniques are detailed in Sections IV and V to develop the *ADAS* system and generate δ_{sw-c}:

- $LPV/\mathscr{H}_\infty$ control technique.
- Super-Twisting Sliding Mode (*STSM*) control technique.

Finally the assistance steering δ^a_{sw-c} is calculated from δ_{sw-c}, after passing the signal through a filter representing the steering actuator.

IV. $LPV/\mathscr{H}_\infty$ *ADAS* System

In this section, a detailed description of the development of the *ADAS* System is presented. The optimal $\mathscr{H}_\infty$ theory based on offline Linear Matrix Inequality (LMI) optimal solution, in the framework of *LPV* systems is used to synthesis this controller. The global multilayer architecture is shown in the Fig. 2. In the control layer, the output variable i.e the vehicle yaw rate $\dot{\psi}$ is fed-back from nonlinear vehicle model and is controlled through an optimal Single-Input-Single-Output *SISO* $LPV/\mathscr{H}_\infty$ controller, in order to realize a trajectory following. For that, a reference yaw rate generator is used to give the desired yaw rate $\dot{\psi}_{ref}$. In addition, ρ is a time-varying scheduling gain/parameter that schedules the assistance objective of the $LPV/\mathscr{H}_\infty$ controller. ρ is implicitly expressed in δ^a_{sw-c} which will be added to the δ_{sw-h} (see Fig. 2). Then, a decision layer (the higher layer)

$$\dot{X} = \begin{bmatrix} \dot{\beta} \\ \ddot{\psi} \end{bmatrix} = \underbrace{\begin{bmatrix} -\frac{C_f+C_r}{mV_x} & -(1+\frac{l_fC_f-l_rC_r}{mV_x^2}) \\ -\frac{l_fC_f-l_rC_r}{I_z} & -\frac{l_f^2C_f+l_r^2C_r}{I_zV_x} \end{bmatrix}}_{A} \begin{bmatrix} \beta \\ \dot{\psi} \end{bmatrix} + \underbrace{\begin{bmatrix} \frac{C_f}{mV_x} \\ \frac{l_fC_f}{I_z} \end{bmatrix}}_{B} \delta_{sw-c} \tag{2}$$

is developed to monitor the driver's behavior. It sends the value of scheduling parameter ρ, based on the parameter λ (discussed later). λ is function of the lateral error (e_y) and driver's availability (DA) (see Fig. 2). So, based on these information, the $LPV/\mathscr{H}_\infty$ controller generates the control steering angle δ_{sw-c} provided by the AFS as an assistance input, while considering actuator constraint (saturation and cut-off frequencies) in the actuator layer.

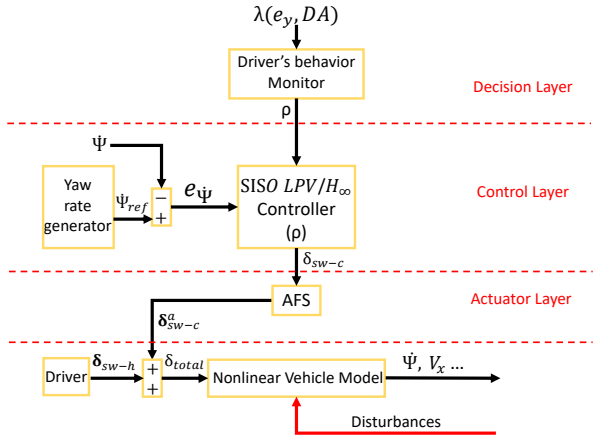

Fig. 2: $LPV/\mathscr{H}_\infty$ *ADAS* system architecture.

A. *Control Layer synthesis:*

The control layer architecture is drawn in Fig. 3. As a standard $\mathscr{H}_\infty$ structure, it contains the controller $K_{LPV/\mathscr{H}_\infty}(\rho)$ to be synthesized, and the generalized plant $\sum_g$, where $\rho(\lambda)$ is a weighted parameter calculated by the decision making monitor to adapt the controller dynamics and performances according to the driving conditions. The controller $K_{LPV/\mathscr{H}_\infty}(\rho)$ has as input, the error between the desired yaw rate on trajectory (given by the reference yaw rate generator) and the actual yaw rate of the vehicle (e_ψ=ψ_{ref}-ψ). Since the $\mathscr{H}_\infty$ approach is a model-based robust control technique, the actual yaw rate is calculated based on the LTI vehicle model of the Section II (*Plant P*).

Plant P of the generalized plant $\sum_g$ is expressed in system (2). It has δ_{sw-c} as AFS control input; and the actual yaw rate $\dot{\psi}$, as output to be controlled. The remaining subsystems of $\sum_g$ i.e. the weighting functions $W_\psi(\rho)$ and $W_\delta(\rho)$ of Fig. 3 are defined to characterize the performance objective Z_1 and the actuators' constraint Z_2. The general form of these weights depends on the simulated vehicle and integrated actuators [10], given as :

- $W_\psi(\rho)$ weights the yaw rate control objective:

$$W_\psi(\rho) = \rho \frac{s/M_1 + 2\pi f_1}{s + 2\pi f_1 A_1} \tag{4}$$

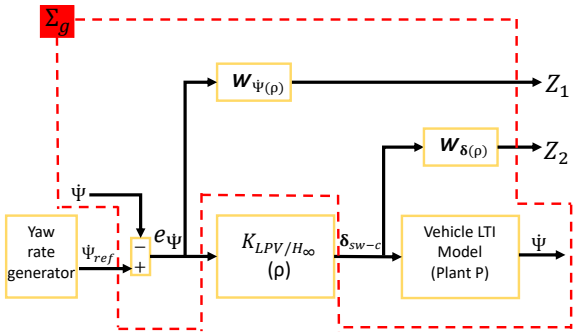

Fig. 3: Control layer architecture.

where M_1 is sufficiently high for a large robustness margin, and A_1 is the tolerated tracking error on e_ψ. $W_\psi(\rho)$ is shaped to reduce the yaw rate error in the range of frequencies below a cut-off frequency f_1 where the vehicle operates [11]. $W_\psi(\rho)$ is linearly parametrized by the varying parameter ρ, where $\rho \in \left\{ \underline{\rho} \leq \rho \leq \overline{\rho} \right\}$ ($\underline{\rho}$ and $\overline{\rho}$ are constants representing the lower and higher values of ρ). When $\rho = \overline{\rho}$, the performance objective e_ψ is prioritized and the *ADAS* System is switched-on, on the contrary, when $\rho = \underline{\rho}$, e_ψ is relaxed, the driver navigates correctly and the assistance is deactivated.

- $W_\delta(\rho)$ weights the steering control input, δ_{sw-c}:

$$W_\delta(\rho) = \frac{1}{\rho} \frac{s + 2\pi f_2/M_2}{\varepsilon_u s + 2\pi f_2} \tag{5}$$

where M_2 is sufficiently high for a large robustness margin, ε_u is concerned with the noise rejection at high frequencies and f_2 is the filter's frequency. This filter forces the steering system to act at this frequency in order to avoid driver annoyance. This filter design is inspired from [12]. The novelty here is the dependency of $W_\delta(\rho)$ on ρ, which allows to promote or penalize the steering depending on all possible situations. For instance, when $\rho = \overline{\rho}$, the driver's behavior is not adequate, and the AFS is promoted to maintain the lane keeping and help the driver. When $\rho = \underline{\rho}$, that means the driver acts appropriately, and the AFS is relaxed. In this case, the driver is the only responsible of driving action.

After determining the subsystems of Fig. 3, $\mathscr{H}_\infty$ control technique is applied in order to minimize the controlled outputs Z_1 and Z_2 for any exogenous input. For more information about the robust $LPV/\mathscr{H}_\infty$ theory, see [13] and [14].

Interconnection between $\sum_g$ subsystems is done using "*sysic*" Matlab function (Robust Control Toolbox). Since the generalized plant $\sum_g$ is LPV [15], it can be formulated as:

$$\Sigma_g(\rho) : \begin{bmatrix} \dot{x} \\ z \\ y \end{bmatrix} = \begin{bmatrix} A(\rho) & B_1(\rho) & B_2(\rho) \\ C_1(\rho) & D_{11}(\rho) & D_{12}(\rho) \\ C_2 & D_{21} & 0 \end{bmatrix} \begin{bmatrix} x \\ w \\ U \end{bmatrix}, \tag{6}$$

where ρ is time-varying scheduling parameter, x includes the state variables of *Plant P* and of the weighting functions, $w = [\dot{\psi}_{ref}]^T$ is the exogenous input, $U = [\delta_{sw-c}]^T$ represents the control input, $y = [\dot{\psi}]^T$ is the measurement vector fed-back to the controller, and $z = [Z_1, Z_2]^T$ is the weighted controlled outputs vector of the generalized plant $\sum_g$.
Note that the matrices B_2, and D_{12} depend on ρ, which is not compatible with $\mathscr{H}_\infty$ requirements for polytopic systems. However, this issue is relaxed using some filter on the control input [16].

Problem resolution: LMI based LPV/$\mathscr{H}_\infty$:

The *LMI* based *LPV*/$\mathscr{H}_\infty$ problem consists in finding the controller $K_{LPV/\mathscr{H}_\infty}(\rho)$, scheduled by the parameter ρ, such that:

$$K_{LPV/\mathscr{H}_\infty}(\rho) : \begin{bmatrix} \dot{x}_c \\ u \end{bmatrix} = \begin{bmatrix} A_c(\rho) & B_c(\rho) \\ C_c(\rho) & 0 \end{bmatrix} \begin{bmatrix} x_c \\ y \end{bmatrix}, \quad (7)$$

This controller aims to minimize the $\mathscr{H}_\infty$ norm of the closed-loop *LPV* system formed by the equations (6) and (7). There are many approaches that exist in the literature to solve this problem such as: polytopic, gridding and Linear Fractional Transformation *LFT* [17]. In the present work, a polytopic approach (see [18]) has been used for controller synthesis. Thanks to the Bounded Real Lemma (*BRL*) extended to *LPV* systems, this controller can be found. According to the system (6) and after a change of basis presented in [18], a non conservative *LMI* that expresses the same problem as *BRL* is formulated in (8). A Semi-Definite Program (*SDP*) (Yalmip/Sedumi solver) has been used to solve the inequalities equations given in (8) (see [19]), while minimizing γ for $\rho = \left\{\underline{\rho}, \overline{\rho}\right\}$ ($\gamma_{optimal} = 1.15$).

According to the polytopic approach, the final controller, $K_{LPV/\mathscr{H}_\infty}(\rho)$, is a convex combination of all controllers calculated at the vertices $\left\{\underline{\rho}, \overline{\rho}\right\}$ [15] such as:

$$K_{LPV/\mathscr{H}_\infty}(\rho) = \frac{|\rho-\overline{\rho}|}{(\overline{\rho}-\underline{\rho})} K_{\mathscr{H}_\infty}(\underline{\rho}) + \frac{|\rho-\underline{\rho}|}{(\overline{\rho}-\underline{\rho})} K_{\mathscr{H}_\infty}(\overline{\rho}), \quad (9)$$

where $K_{\mathscr{H}_\infty}(\underline{\rho})$ and $K_{\mathscr{H}_\infty}(\overline{\rho})$ are the solutions of the polytopic problem at each vertex.

Yaw rate generator at a look-ahead distance:

The reference yaw rate generator is developed at a look-ahead distance l_s in front of the vehicle, in order to generate a reference yaw-rate $\dot{\psi}_{ref}$ to the *LPV*/$\mathscr{H}_\infty$ controller for the trajectory following purpose. This controller aims that $\dot{\psi}$ follows $\dot{\psi}_{ref}$ in order to keep the lane with a high accuracy. For that, the reference yaw rate generator uses the current vehicle's speed V_x and the information from the map matching e_{y-l_s} to calculate $\dot{\psi}_{ref}$. Refer to [20], $\dot{\psi}_{ref}$ can be approximated as:

$$\dot{\psi}_{ref} = \frac{-2V_x e_{y-l_s}}{l_s^2} \quad (10)$$

where e_{y-l_s} is the vehicle lateral error at a look-ahead distance l_s, w.r.t the trajectory.

B. Decision Layer: ρ calculation

The decision layer is developed to adjust the controller according to the driver's behavior. This layer delivers the scheduling parameter ρ depending on the parameter λ.
Let us introduce the parameter λ function of the lateral error of the vehicle e_y w.r.t the trajectory at the center of gravity of the vehicle (*CG*) and the driver's availability (*DA*). *DA* $\in [0,1]$ is a dynamic variable related to the driver. *DA*=1 corresponds to a full driver's confidence. It can be calculated based on different factors: driver's eyes analysis, driver's head position, level of driver's sleepiness, etc. Therefore, the calculation of diver's availability is not in the scope of this work and it is considered as an input given by a diagnosis module to this layer. λ is expressed as:

$$\lambda = |e_y| + (1 - DA) \quad (11)$$

As shown in the equation (11), λ depends on e_y and *DA*. Two rules for λ are defined as follows:
* When $\lambda \leq \underline{\lambda}$, that means $|e_y| \leq \underline{e_y}$ and *DA*=1, then no need to assist the driver during this driving maneuver, and the assistance system (*AFS*) should be switched-off. The driver is in normal driving situation and he is available.
* When $\lambda \geq \overline{\lambda}$, that means $|e_y| \geq \overline{e_y}$ and/or *DA* is simply low (*DA*=0), then the *ADAS* System (*AFS*) should be switched-on in order to compensate the driver's error and unavailability.
Referring to this analysis, the scheduled gain ρ feeds the *LPV*/$\mathscr{H}_\infty$ controller with the sufficient information about the weights to be pushed or attenuated. The relation between ρ and λ is presented by a "*sigmoid*" function (12) (see Fig. 4).

$$\rho = \underline{\rho} + \frac{\overline{\rho} - \underline{\rho}}{1 + e^{-\frac{8}{\overline{\lambda}-\underline{\lambda}}(\lambda - \frac{\overline{\lambda}+\underline{\lambda}}{2})}} \quad (12)$$

C. Actuator Layer

The actuator layer includes the *AFS* actuator used to generate the physical input of the system. The *AFS* is an electrical motor which provides the added steering angle δ^a_{sw-c}. In order to ensure that the *AFS* actuator is able to provide the added steering angle demanded by the controller δ_{sw-c}, the *AFS* is modeled as follows:

$$\dot{\delta}^a_{sw-c} = 2\pi f_2(\delta_{sw-c} - \delta^a_{sw-c}) \quad (13)$$

where δ^a_{sw-c} follows δ_{sw-c}, f_2 is the actuator cut-off frequency. This actuator is bounded between $\left[-\delta^a_{sw-c,max}, +\delta^a_{sw-c,max}\right]$, with $\delta^a_{sw-c,max}$ the maximum amount of steering angle that can be added by the *AFS* actuator for assistance purpose.

V. Super-Twisting Sliding Mode (*STSM*) *ADAS* System

The global multilayer architecture is shown in the Fig. 5. The main difference between both architectures is in the control layer, where the *AFS* control input δ_{sw-c} is dedicated to control the lateral error e_y by using the Super-Twisting Sliding Mode (*STSM*) control technique to realize a lane

$$\begin{bmatrix} A(\rho)X + XA(\rho)^T + B_2\widetilde{C}(\rho) + \widetilde{C}(\rho)^T B_2^T & (*)^T & (*)^T & (*)^T \\ \widetilde{A}(\rho) + A(\rho)^T & YA(\rho) + A(\rho)^T Y + \widetilde{B}(\rho)C_2 + C_2^T \widetilde{B}(\rho)^T & (*)^T & (*)^T \\ B_1(\rho)^T & B_1(\rho)^T Y + D_{21}^T \widetilde{B}(\rho)^T & -\gamma I & (*)^T \\ C_1(\rho)X + D_{12}\widetilde{C}(\rho) & C_1(\rho) & D_{11}(\rho) & -\gamma I \end{bmatrix} < 0 \text{ and } \begin{bmatrix} X(\rho) & I \\ I & Y(\rho) \end{bmatrix} > 0. \tag{8}$$

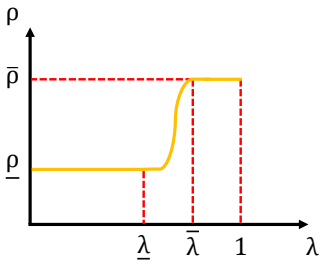

Fig. 4: Scheduling parameter ρ function of the decision parameter λ

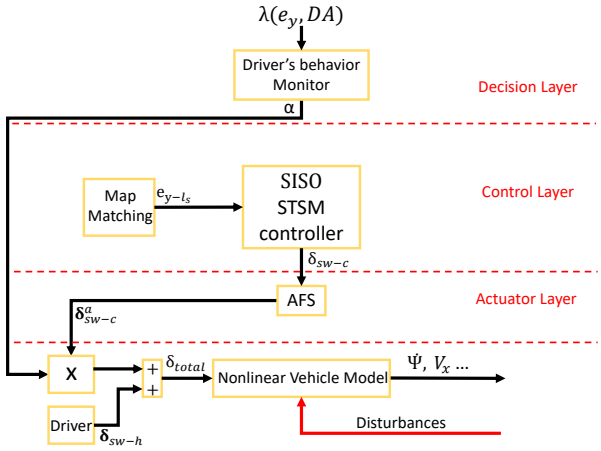

Fig. 5: Super-Twisting Sliding Mode ($STSM$) ADAS system architecture.

following. The Map matching aims to localize the vehicle position on the reference map by calculating the lateral error at l_s look-ahead distance w.r.t the trajectory. Finally, the decision layer is developed to generate the percentage of assistance α based on λ.

A. Control & Decision Layers:

The control layer consists of a single-input, single-output ($SISO$) $STSM$ controller that controls the lateral error at a look-ahead distance l_s to realize a lane keeping. The control input is the steering wheel angle δ_{sw-c} for the lateral dynamics. The longitudinal movement for both architectures is realized also using a $STSM$ controller. Note that the $STSM$ control technique is one of the most robust control techniques that suit our control problem. The main idea of the $STSM$ is to define a sliding surface, representing the desired behavior of the system, where the dynamic states are forced to reach this surface during a finite time and remain on it. Consider the second order system given as:

$$\dot{X} = f(X,t) + g(X,t)u(t) \tag{14}$$

where $X = [x, \dot{x}]^T \in \Re^2$ is the state vector, u is the control input, and f, g are continuous non-linear functions. X^* is the desired state of X with $X^* = [x^*, \dot{x}^*]^T \in \Re^2$. The error vector is given by $E = X - X^* = [e, \dot{e}]^T \in \Re^2$ where $e = x - x^*$ and $\dot{e} = \dot{x} - \dot{x}^*$. Therefore, a sliding variable s with relative degree $r = 1$ w.r.t the control input, is defined as:

$$s = \dot{e} + \lambda\ e. \tag{15}$$

The second order derivative of s can be written in the form:

$$\ddot{s}(s,t) = \Phi(s,t) + \xi(s,t)\dot{u}(t) \tag{16}$$

where $\Phi(s,t)$ and $\xi(s,t)$ are bounded functions.
The goal of the Super-Twisting algorithm is to enforce the sliding variable s to converge to zero ($s = 0$) in finite time. Assume that there exist positive constants S_0, b_{min}, b_{max}, C_0, U_{max} verifying for all $X \in \Re^n$ and $|s(X,t)| < S_0$:

$$\begin{cases} |u(t)| \leq U_{max} \\ |\Phi(s,t)| < C_0 \\ 0 < b_{min} \leq |\xi(s,t)| \leq b_{max} \end{cases} \tag{17}$$

Thus, the control input based on the Super-Twisting Sliding Mode algorithm [21], is given as:

$$u(t) = u_1 + u_2 \begin{cases} u_1 = -\alpha_1 |s|^\tau \text{sign}(s), \ \ \tau \in]0, 0.5] \\ \dot{u}_2 = -\alpha_2 \text{sign}(s) \end{cases} \tag{18}$$

α_1 and α_2 are positive gains. The following conditions guarantee the finite time convergence:

$$\begin{cases} \alpha_1 \geq \sqrt{\frac{4C_0(b_{max}\alpha_2 + C_0)}{b_{min}^2(b_{min}\alpha_2 - C_0)}} \\ \alpha_2 > \frac{C_0}{b_{min}} \end{cases} \tag{19}$$

The convergence analysis is shown in [22].
The controller synthesis is based on a robotic formalism model presented in [23], that represents the coupling between the longitudinal and lateral dynamics. Based on this model, we choose the two sliding variables for the longitudinal and lateral controllers as follows:

$$\begin{aligned} s_1 &= e_{Vx} + \lambda_x \int e_{Vx},\ \lambda_x > 0 \\ s_2 &= \dot{e_y} + \lambda_y e_y, \qquad \lambda_y > 0 \end{aligned} \tag{20}$$

where λ_x and λ_y are positive constants, and, e_{Vx} (e_{Vx}= V_x-V_x^*) and e_y are the vehicle longitudinal speed error and the lateral error respectively. The sliding variables s_1 and s_2 have a relative degree equal to one w.r.t the inputs respectively, the driving/braking torque Γ_c for the longitudinal dynamics and

the steering angle δ_{sw-c} for the lateral dynamics. Thus, in order to converge these variables to zero and the controlled states follow the desired ones, and based on the above discussion, the torque and the steering angle control applied to the vehicle, are given by:

$$\Gamma_c = -\alpha_{\Gamma_c,1}|s_1|^{\tau_{\Gamma_c}} sign(s_1) - \alpha_{\Gamma_c,2}\int_0^t sign(s_1)d\tau,$$
$$\delta_{sw-c} = u_1 + u_2 \quad \begin{cases} u_1 = -\alpha_{\delta,1}|s_2|^{\tau_\delta} sign(s_2), \\ u_2 = -\alpha_{\delta,2}\int_0^t sign(s_2)d\tau, \end{cases} \tag{21}$$

where $\alpha_{\delta,i}$ and $\alpha_{\Gamma_c,i}$ with $i = [1, 2]$, are positive constants satisfying the conditions in (19). τ_{Γ_c} and τ_δ are constants in $]0, 0.5]$. The function *sign* is smoothed by the approximation $sign(s_1) = \frac{s}{|s|+\varepsilon_x}$ and $sign(s_2) = \frac{s}{|s|+\varepsilon_y}$, where ε_x and ε_y are positive small values.

Similar as before, a decision layer monitors the driver's behavior through λ (function of e_y and DA). It calculates and sends instantly the value of α, the fusion parameter, depending on the parameter λ (given in IV-B) in order to promote/attenuate the intervention of *ADAS* System in the driving maneuver.

* When $\lambda \leq \underline{\lambda}$, α is equal to 0 and the *ADAS* System (*AFS*) is attenuated because the driver operates without any errors.
* When $\lambda \geq \overline{\lambda}$, the driver is no more available and distracted, then an assistance input (*AFS*) is needed to be switched-on to compensate the driver's error, and α is equal to 1.

"*Sigmoid*" function (22) (see Fig. 6) governs the relation between α and λ, to ensure a smooth and continuous variation of α. Finally, the actuator layer developed in the section IV-C, is used to generate the physical input δ^a_{sw-c} of the system.

$$\alpha = \frac{1}{1 + e^{-\frac{8}{\overline{\lambda}-\underline{\lambda}}(\lambda - \frac{\overline{\lambda}+\underline{\lambda}}{2})}} \tag{22}$$

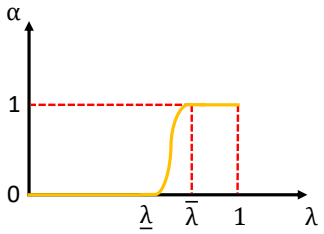

Fig. 6: Scheduling parameter α

VI. Controllers' validation

The proposed $LPV/\mathscr{H}_\infty$ and Super-Twisting Sliding Mode (*STSM*) controllers are validated in this section. Validation is done by simulation using Matlab/Simulink with a complete nonlinear model of the vehicle, validated on "*SCANeR Studio*" simulator. Then, a comparison is done between both controllers in order to show the difference in terms of performance and effectiveness of each control technique. The different parameters numerical values of the two controllers used during the simulation are given in Table I.

A. Simulation results

As mentioned before, this section is dedicated to validate and compare the proposed $LPV/\mathscr{H}_\infty$ and the *STSM* controllers. A scenario is chosen in the way that the driver realizes a path following maneuver at speed 60 Km/h (see Fig. 12) on the track given in the Fig. 7. However, during this maneuver, sudden errors are injected on the driver's behavior between $35s$ and $50s$ and between $70s$ and $85s$ respectively where the driver is no more available. The vehicle is deviated from the centerline of the road. Thus, an *ADAS* system represented by one of both proposed controllers, is switched-on in order to compensate the driver's error and avoid a dangerous situation. In this scenario, the comparison is done when the driver drives his vehicle without *ADAS* (alone) and by integrating the proposed controllers i.e the $LPV/\mathscr{H}_\infty$ and the *STSM* controller into the vehicle (driving with *ADAS* System). This scenario shows the advantage of having an *ADAS* system implemented in the vehicle for a lane keeping maneuver. The two proposed *ADAS* system controllers monitor and supervise the vehicle situation and interact if necessary in order to compensate the inappropriate driver's action. The results are presented in the following to show the effectiveness of the developed *ADAS* systems to help the driver during the lane keeping maneuver. The Fig.

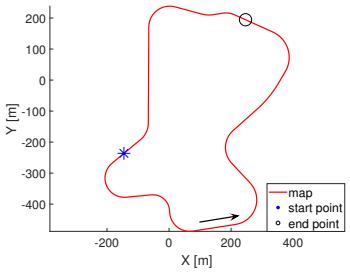

Fig. 7: Map of the tracked trajectory

TABLE I: Controller's Parameters for Simulation

Parameters	Values
$M_1; M_2; A_1$	$2; 1; 0.1 = 10\%$
$f_1; f_2$	$5\ Hz; 10\ Hz$
$\underline{\rho}; \overline{\rho}; \underline{e_y}; \overline{e_y}; \underline{\lambda}; \overline{\lambda}$	$0.01; 0.2; 0.3; 0.5; 0.3; 0.5$
$\delta^a_{sw-c,max}; \varepsilon_u; l_s$	$5°; 0.01; 3$
$\lambda_x; \lambda_y; \varepsilon_x; \varepsilon_y$	$0.01; 8; 0.1; 1$
$\alpha_{\delta,1}; \tau_\delta; \alpha_{\delta,2}$	$0.1; 0.5; 0.01$
$\alpha_{\Gamma_c,1}; \tau_{\Gamma_c}; \alpha_{\Gamma_c,2}$	$500; 0.5; 5$

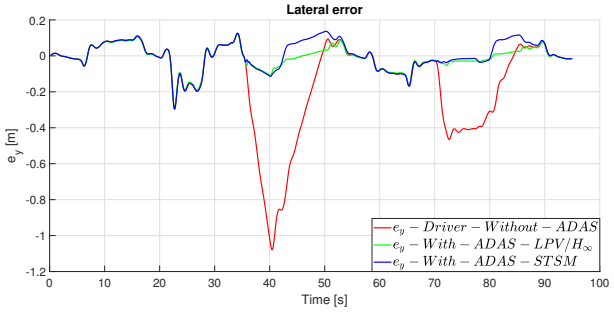

Fig. 8: The lateral error

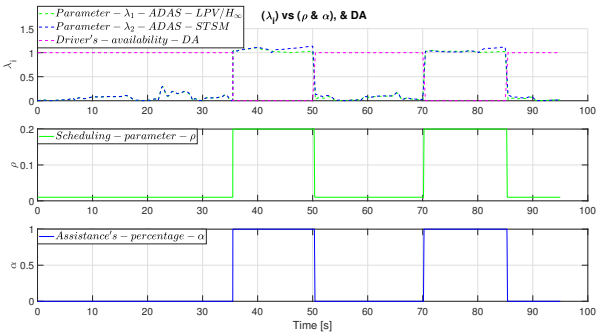

Fig. 9: λ_i vs (ρ & α) & DA

Fig. 10: The different steering wheel angles

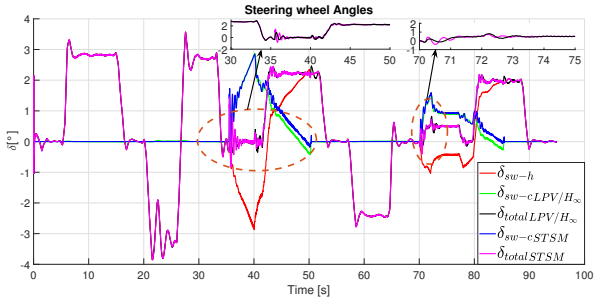

Fig. 11: The different total steering wheel angles

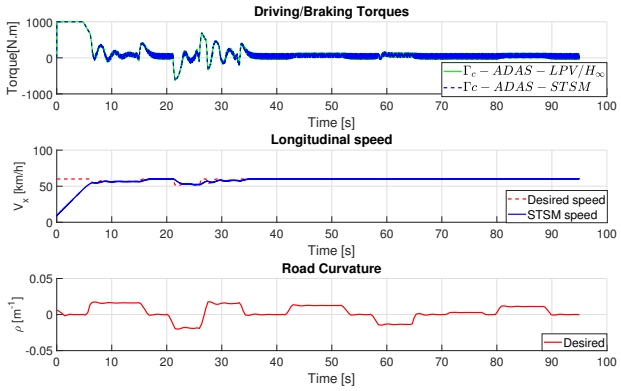

Fig. 12: Driving/braking torque vs Vehicle dynamic variables

8 shows the lateral error w.r.t the trajectory of: driver without *ADAS*, driving with *ADAS* $LPV/\mathscr{H}_\infty$ and driving with *ADAS* $STSM$. As we can see, the error is injected at $35s$ on the driver's behavior and both *ADAS* Systems ($LPV/\mathscr{H}_\infty$ and $STSM$ controllers) diminish this error (initially $1m$) caused by the driver on the curvy road (see Fig. 12). Thus, they have achieved the assistance goal with a high accuracy of lane keeping (e_y between $-25cm$ and $20cm$, Fig. 8). They are switched-on until t=50s, where $\lambda \geq \overline{\lambda}$ (for the following, we consider λ_1 for $LPV/\mathscr{H}_\infty$ and λ_2 for $STSM$) because the driver is not available (DA=0) and the lateral error is more than $\overline{e_y}$ (see Fig. 9). Remember that the DA is an input to our system given by a diagnosis module in order to determine the driver's status. We consider that the error of the driver is detected with $0.5s$ of delay. Again at t=70s, an *ADAS* System is still needed because there is a second error caused by the driver's behavior and $DA = 0$ again. This system assists the driver until t=85s. At t=85s, the driver's behavior returned normal and he is available again to act on the vehicle's lateral control without any help. The assistance objective can be explained by observing the decision layer of each *ADAS* system architecture, in other words, the monitoring criterion λ. Fig. 9 shows the two parameters λ_1 and λ_2, with the corresponding scheduling gain ρ of the $LPV/\mathscr{H}_\infty$ *ADAS* system architecture and the percentage of assistance α of the $STSM$ *ADAS* system architecture, and, the driver's availability DA. For $\lambda_1 \geq \overline{\lambda}$ (resp. $\lambda_2 \geq \overline{\lambda}$), which means that the driver is not available and there is an error on his behavior, both *ADAS* systems have switched-on to assist and help him, and remain the vehicle stable. In this case, corresponding to $DA = 0$ and/or e_y more than $\overline{e_y}$, especially between $35s$ and $50s$ and between $70s$ and $85s$, the scheduling gain ρ of the $LPV/\mathscr{H}_\infty$ (resp. the percentage of assistance α of the $STSM$) is set to $\rho = \overline{\rho}$ (resp. $\alpha = 1$), which activates the assistance. For the region, when $\lambda_1 \leq \underline{\lambda}$ (resp. $\lambda_2 \leq \underline{\lambda}$), the scheduling gain ρ (resp. the percentage of assistance α) is set to $\rho = \underline{\rho}$ (resp. $\alpha = 0$), which means the driver is available and acts correctly and the *ADAS* system is Switched-off (see Fig. 9). Based on this discussion, one can conclude that the *ADAS* System is switched-on when it is needed in order to assist the driver and ensure lane keeping. Referring to the Fig. 8 and 9, the two *ADAS* systems have almost the same behavior and they are able to help the driver by compensating his errors. Fig. 10 shows the driver steering angle δ_{sw-h} and the assistance AFS steering angles δ_{sw-c} of the $LPV/\mathscr{H}_\infty$ and the $STSM$ *ADAS* System respectively, on the steering wheels. Refer to this figure, both controllers ($\delta_{sw-cLPV/H_\infty}$ and $\delta_{sw-cSTSM}$) are in conflict with the human driver δ_{sw-h} (the red curve) between $35s$ and $50s$ and between $70s$ and $85s$ in order to compensate his errors. In addition, we can notice that both controllers provide almost the similar steering angle (the green and blue curves have almost the same behavior), with some additional oscillations of $STSM$ controller compared to the $LPV/\mathscr{H}_\infty$ controller. To show the difference between the two controllers, both total steering angles for lateral displacement: $\delta_{totalLPV/H_\infty}$ and $\delta_{totalSTSM}$, are presented in Fig. 11. The oscillations appear more with the $STSM$ than the $LPV/\mathscr{H}_\infty$ controller, which correspond to the main known drawback of the $STSM$ approach. However, there are some oscillations in the $LPV/\mathscr{H}_\infty$

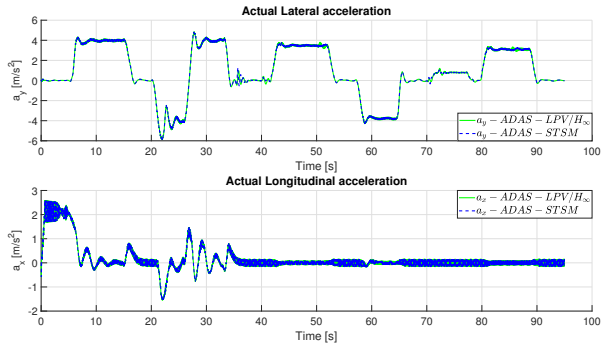

Fig. 13: The vehicle dynamic variables

but with small peak values (see Fig. 11). Fig. 12 shows the longitudinal *STSM* motor torque in case of both *ADAS* controllers, the longitudinal speed tracking of the desired one through the *STSM* controller and the road curvature of the desired trajectory. Remember that the longitudinal displacement is achieved by a *STSM* controller for both *ADAS* system architectures. Finally, Fig. 13 shows the lateral and longitudinal accelerations. The lateral acceleration does not exceed the $\pm 4m/s^2$, which demonstrate a comfortable and stable driving zone. In addition, the actual longitudinal acceleration is pertinent ($< \pm 2m/s^2$) for a comfortable maneuver. To conclude based on the results discussed above, the *STSM* control technique is simple and robust with high performance and low cost. However, its main drawback is the oscillations and chattering. Concerning the $LPV/\mathscr{H}_\infty$ control technique, it is optimal and robust with high performance in terms of reducing chattering and oscillations. Nonetheless, it is a complex and costly control method.

VII. Conclusion and Perspectives

To conclude, in this paper two *ADAS* systems have been developed for the Lane Keeping to assist the driver and enhance driving safety. This assistance objective is done by developing a Fusion block, where the fusion parameter is calculated through a decision layer to determine the percentage of assistance. The different Driving modes are detailed in this work. The development of both *ADAS* controllers is done using the $LPV/\mathscr{H}_\infty$ and the Super-Twisting Sliding Mode (*STSM*) control approaches. The different layers including the decision layer for the decision making process are detailed. The proposed *ADAS* controllers are validated in Matlab/Simulink for a given scenario with a complete nonlinear model of the vehicle, validated on "*SCANeR Studio*" (OKtal) simulator. In addition, a comparison between both controllers is done. The results show the effectiveness and the performance of the proposed two approaches in terms of driver's error compensation and undesirable driving situation prevention. In the future work, we will consider other criteria to prove the effectiveness and the performance of the decision making process, integrate the Direct Yaw Control (*DYC*) to enhance vehicle's stability target and validate the approaches on the "*SCANeR Studio*" simulator, connected to a hardware-in-the-loop steering system.

References

[1] F. M. Favarò, N. Nader, S. O. Eurich, M. Tripp, and N. Varadaraju, "Examining accident reports involving autonomous vehicles in california," *PLoS one*, vol. 12, no. 9, p. e0184952, 2017.

[2] V. K. Kukkala, J. Tunnell, S. Pasricha, and T. Bradley, "Advanced driver-assistance systems: A path toward autonomous vehicles," *IEEE Consumer Electronics Magazine*, vol. 7, no. 5, pp. 18–25, 2018.

[3] C. Sentouh, S. Debernard, J.-C. Popieul, and F. Vanderhaegen, "Toward a shared lateral control between driver and steering assist controller," *IFAC Proceedings Volumes*, vol. 43, no. 13, pp. 404–409, 2010.

[4] A.-T. Nguyen, C. Sentouh, and J.-C. Popieul, "Driver-automation cooperative approach for shared steering control under multiple system constraints: Design and experiments," *IEEE Transactions on Industrial Electronics*, vol. 64, no. 5, pp. 3819–3830, 2016.

[5] G. Perozzi, C. Sentouh, J. Floris, and J.-C. Popieul, "On nonlinear control for lane keeping assist system in steer-by-wire road wheeled vehicles," 07 2020.

[6] C. Sentouh, B. Soualmi, J.-C. Popieul, and S. Debernard, "Cooperative steering assist control system," in *2013 IEEE international conference on systems, man, and cybernetics*. IEEE, 2013, pp. 941–946.

[7] F. Borroni and M. Tanelli, "A weighting approach to the shared-control of lateral vehicle dynamics," *IFAC-PapersOnLine*, vol. 51, no. 9, pp. 305–310, 2018.

[8] A. Li, Y. Chen, W.-C. Lin, and X. Du, "Shared steering control of tire blowout for ground vehicles," in *2020 American Control Conference (ACC)*. IEEE, 2020, pp. 4862–4867.

[9] A. Hamdan, R. Talj, and V. Cherfaoui, "A fuzzy logic shared steering control approach for semi-autonomous vehicle," in *2021 20th International Conference on Advanced Robotics (ICAR)*. IEEE, 2021, pp. 83–90.

[10] M. Doumiati, A. Victorino, R. Talj, and A. Charara, "Robust lpv control for vehicle steerability and lateral stability," in *53rd IEEE Conference on Decision and Control, pp. 4113–4118*, 2014.

[11] B. Heißing and M. Ersoy, *Chassis handbook: fundamentals, driving dynamics, components, mechatronics, perspectives*. Springer Science & Business Media, 2010.

[12] H. Atoui, V. Milanés, O. Sename, and J. J. Martinez, "Real-time look-ahead distance optimization for smooth and robust steering control of autonomous vehicles," in *2021 29th Mediterranean Conference on Control and Automation (MED)*. IEEE, 2021, pp. 924–929.

[13] O. Sename, P. Gaspar, and J. Bokor, *Robust control and linear parameter varying approaches: application to vehicle dynamics*. Springer, vol. 437, 2013.

[14] D.-W. Gu, P. Petkov, and M. M. Konstantinov, *Robust control design with MATLAB®*. Springer Science & Business Media, 2005.

[15] P. Apkarian, P. Gahinet, and G. Becker, "Self-scheduled $h\infty$ control of linear parameter-varying systems: a design example," *Automatica*, vol. 31, no. 9, pp. 1251–1261, 1995.

[16] P. Apkarian and P. Gahinet, "A convex characterization of gain-scheduled $h\infty$ controllers," *IEEE Transactions on Automatic Control*, vol. 40, no. 5, pp. 853–864, 1995.

[17] A. Zin, "Sur la commande robuste de suspensions automobiles en vue du contrôle global de châssis." Ph.D. dissertation, Institut National Polytechnique de Grenoble-INPG, 2005.

[18] C. Scherer, P. Gahinet, and M. Chilali, "Multiobjective output-feedback control via lmi optimization," *IEEE Transactions on automatic control*, vol. 42, no. 7, pp. 896–911, 1997.

[19] M. Doumiati, O. Sename, L. Dugard, J.-J. Martinez-Molina, P. Gaspar, and Z. Szabo, "Integrated vehicle dynamics control via coordination of active front steering and rear braking," *European Journal of Control*, vol. 19, no. 2, pp. 121–143, 2013.

[20] H.-S. Tan and J. Huang, "Design of a high-performance automatic steering controller for bus revenue service based on how drivers steer," *IEEE Transactions on Robotics*, vol. 30, no. 5, pp. 1137–1147, 2014.

[21] J. Rivera, L. Garcia, C. Mora, J. J. Raygoza, and S. Ortega, "Super-twisting sliding mode in motion control systems," *Sliding mode control*, pp. 237–254, 2011.

[22] V. Utkin, "On convergence time and disturbance rejection of super-twisting control," *IEEE Transactions on Automatic Control*, vol. 58, no. 8, 2013.

[23] A. Chebly, "Trajectory planning and tracking for autonomous vehicles navigation," Ph.D. dissertation, Université de Technologie de Compiègne, 2017.